JACS
JOURNAL OF THE AMERICAN CHEMICAL SOCIETY
pubs.acs.org/JACS
Article

Pinwheel-Shaped Tetranuclear Organoboron Catalysts for Perfectly Alternating Copolymerization of CO_2 and Epichlorohydrin

Guan-Wen Yang, Cheng-Kai Xu, Rui Xie, Yao-Yao Zhang, Xiao-Feng Zhu, and Guang-Peng Wu*

Cite This: J. Am. Chem. Soc. 2021, 143, 3455−3465
Read Online
ACCESS | Metrics & More | Article Recommendations | Supporting Information

ABSTRACT: The copolymerization of carbon dioxide (CO_2) and epoxides to produce aliphatic polycarbonates is a burgeoning technology for the large-scale utilization of CO_2 and degradable polymeric materials. Even with the wealth of advancements achieved over the past 50 years on this green technology, many challenges remain, including the use of metal-containing catalysts for polymerization, the removal of the chromatic metal residue after polymerization, and the limited practicable epoxides, especially for those containing electron-withdrawing groups. Herein, we provide kinds of pinwheel-shaped tetranuclear organoboron catalysts for epichlorohydrin/CO_2 copolymerization with >99% polymer selectivity and quantitative CO_2 uptake (>99% carbonate linkages) under mild conditions (25−40 °C, 25 bar of CO_2). The produced poly(chloropropylene carbonate) has the highest molecular weight of 36.5 kg/mol and glass transition temperature of 45.4 °C reported to date. The energy difference (ΔE_a = 60.7 kJ/mol) between the cyclic carbonate and polycarbonate sheds light on the robust performance of our metal-free catalyst. Control experiments and density functional theory (DFT) calculations revealed a cyclically sequential copolymerization mechanism. The metal-free feature, high catalytic performance under mild conditions, and no trouble with chromaticity for the produced polymers imply that our catalysts are practical candidates to advance the CO_2-based polycarbonates.

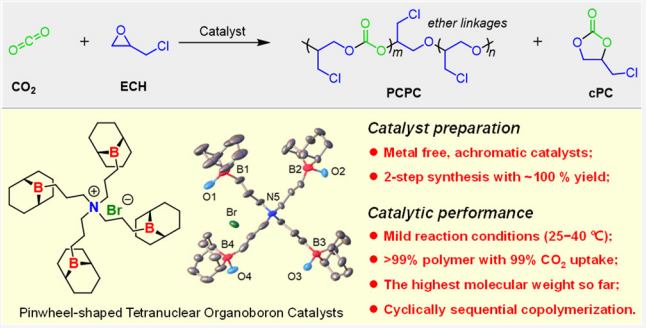

INTRODUCTION

The development of efficient and green techniques for the chemical transformation of CO_2, the major greenhouse gas, into industrially viable products has awakened a global awareness.[1−6] Among various strategies for the chemical utilization of CO_2 being investigated, the construction of degradable CO_2-based polycarbonates (CO_2-PCs) via alternating copolymerization of CO_2 with energy-rich epoxides is an intriguing, practical service platform,[3,7−9] which was pioneered by Inoue and co-workers in 1969.[10,11] Driven by the deep research on a mechanistic understanding of the copolymerization process, especially by developing a highly active catalyst,[12−27] attempts at the industrialization of CO_2/epoxide-derived copolymers are visible in several places in the world.[28,29] Encouragingly, the life cycle assessment of CO_2-PC-derived polymeric materials demonstrated that the incorporation of 1 kg of CO_2 into the polymer could reduce 3 kg of CO_2 greenhouse gas emissions, further sparking the interest of academic and industrial circles in this CO_2-derived copolymers.[30,31] Even with the significant advancements achieved over the past 50 years, many challenges remain in the copolymerization of CO_2 with epoxides: e.g., the sophisticated synthesis of the metallic catalysts involved, the cumbersome removal of the metal residue in the products, and the restricted practicable epoxides.

Currently, the vast majority of the CO_2-PCs have been produced from aliphatic epoxides that have electron-donating substituents, as exemplified by propylene oxide (PO), cyclohexene oxide (CHO), and their derivatives.[32,33] In contrast, very limited successful examples have been shown concerning the synthesis of CO_2-PCs using epoxides with electron-withdrawing groups, such as epichlorohydrin (ECH) (Figure 1a). As an central C3 chemical intermediate, ECH has a wide range of applications in rubber, adhesives, ion-exchange resins, and pharmaceutical intermediates with a production of up to ∼2 million tonnes per year.[34] Notably, a fourth of the current global production of ECH is now produced from vegetable glycerin by Solvay and Dow using bio-based industrial processes.[35] From the perspective of polymerization, it is also intriguing to use ECH as a comonomer to construct CO_2-PC, since the introduction of chlorine into polymer backbones can impart rigidity to improve its physical properties, to equip the materials with the fire-retardant ability,

Received: November 29, 2020
Published: February 16, 2021

https://dx.doi.org/10.1021/jacs.0c12425
J. Am. Chem. Soc. 2021, 143, 3455−3465

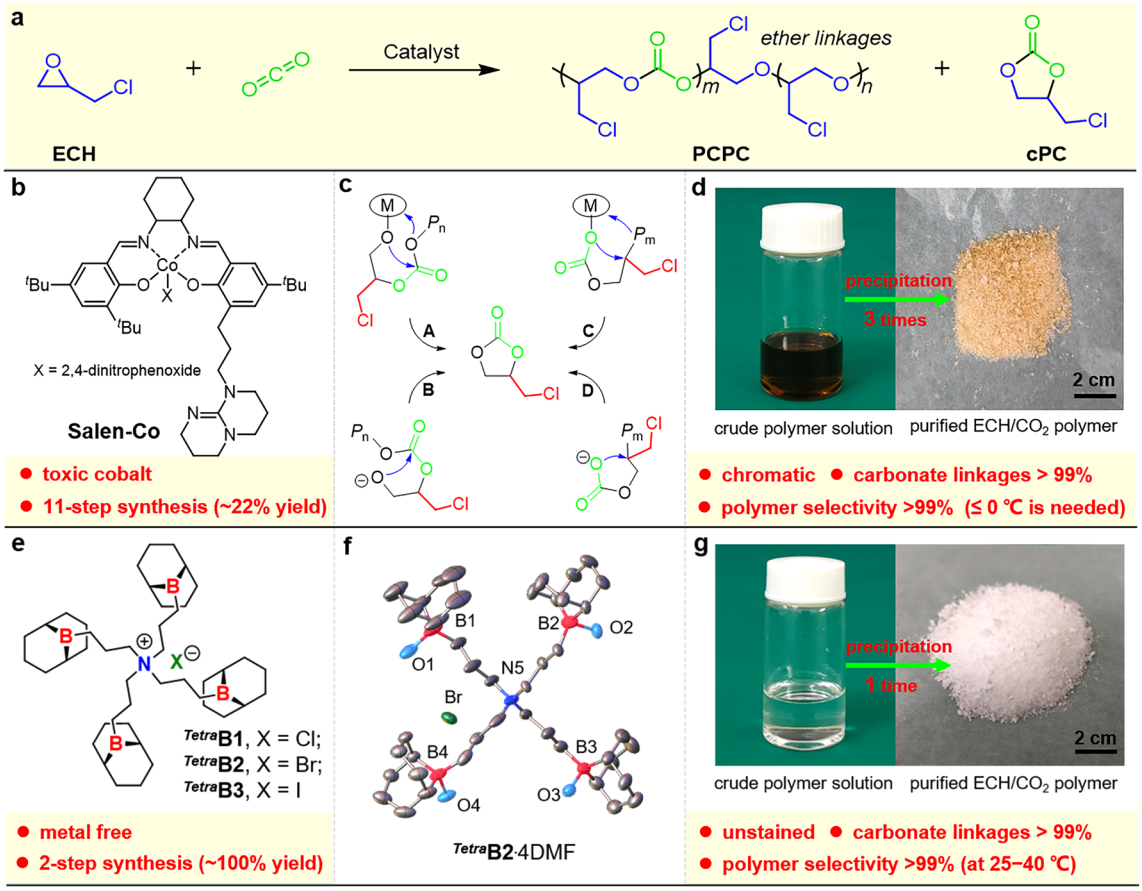

Figure 1. Copolymerization and the high-selectivity catalysts involved. (a) Coupling of ECH and CO_2 to yield PCPC and cPC. (b) The state-of-the-art **Salen-Co** complex for ECH/CO_2 copolymerization. (c) The alkoxy backbiting pathways (A and B) and carbonate backbiting pathways (C and D) leading to the formation of undesired cyclic carbonates. P_n and P_m present alkyl and carbonate substituents, respectively. (d) Photographs of the representative crude polymer solution (in 5 mL of CH_2Cl_2) and the purified polymer after three dissolution−precipitation cycles using the catalyst **Salen-Co**. (e) The tetranuclear organoboron catalysts in this work. (f) The crystal structure of ^{Tetra}**B2**·4DMF, where all the H atoms and solvent molecules are omitted and the coordinated DMF is truncated for clarity. (g) Photographs of the representative crude polymer solution (in 5 mL of CH_2Cl_2) and the purified ECH/CO_2 copolymer using the catalyst ^{Tetra}**B2**.

and to provide postpolymerization sites for new material design with the desired functionalities.[36,37] In fact, the exploration of copolymerization of ECH/CO_2 to produce poly(chloropropylene carbonate) (PCPC) has never stopped since the date of CO_2-PC birth. The first attempt of the ECH/CO_2 copolymerization was also disclosed by Inoue using a heterogeneous catalyst system of diethyl zinc/H_2O that is effective for the copolymerization of PO/CO_2; unfortunately, only <1% PCPC was obtained even when the the reaction time was prolonged to 48 h for ECH/CO_2 copolymerization.[10] In 1994, Shen and co-workers presented a kind of heterogeneous rare-earth-metal catalyst system for the copolymerization of ECH and CO_2, but only <30% carbonate linkages was produced in the obtained poly(carbonate-*co*-ether) materials.[38] In 2013, Zhang et al. reported a Zn-Co(III) double-metal cyanide complex for the copolymerization, affording polymers with a carbonate content of up to 70.7%.[36] Three years later, the carbonate content was increased to 83.1% by the Yoon group using zinc glutarate as the catalyst.[39] A landmark improvement in this sector was made in 2011 by Darensbourg and Lu, who used the homogeneous bifunctional salen-Co(III) catalysts (**Salen-Co**, Figure 1b) and produced a completely alternating copolymer of CO_2 and ECH for the first time.[40] It is worth noting that a low temperature (0 °C) was necessary to suppress the production of the thermally stable byproduct, cyclic carbonate (cPC); otherwise, a considerable amount of cPC (28%) was generated if the polymerization was conducted at 25 °C. The quite small difference in activation energy (ΔE_a = 45.4 kJ/mol) between PCPC and cPC formation rationally explains the fact that the selective synthesis of a copolymer of ECH/CO_2 is more challenging in comparison with the conventional copolymerization processes of PO/CO_2 (ΔE_a = 53.5 kJ/mol).[40] This small energy difference arises from the electron-withdrawing chloromethyl group and leads to a strong tendency for cPC byproduct formation rather than the PCPC, because the alkoxy backbiting (routes A and B in Figure 1c) and carbonate backbiting (routes C and D in Figure 1c) pathways are susceptible to occur during the copolymerization of ECH/CO_2. This explanation clarifies why cPC is usually the sole product for the coupling of ECH and CO_2 using the extensively studied metal compounds (such as Zn, Cr, etc.), which have high polymer selectivity in the conventional copolymerization of CHO/CO_2 or/and PO/CO_2 within broad temperature and pressure windows.[41−43] Despite the fact that **Salen-Co** has enabled the successful synthesis of PCPC with a perfect alternating structure, the time-consuming synthesis of the catalyst (11-step synthetic procedure with ∼22% total yield), the need to remove the chromatic, toxic cobalt residue

https://dx.doi.org/10.1021/jacs.0c12425
J. Am. Chem. Soc. 2021, 143, 3455−3465

Table 1. ECH/CO_2 Copolymerization Results[a]

entry	cat.	mon./cat.	time (h)	temp (°C)	conversn[b] (%)	TON[b]	TOF[b]	selectivity[b] (polymer %)	carbonate linkages (%)[b]	M_n[c] (kg/mol)	$Đ$[c]
1	^{Tetra}**B1**	500	24	25	36.1	180	7.5	>99	>99	16.3	1.19
2	^{Tetra}**B2**	500	24	25	39.6	198	8.3	>99	>99	20.6	1.13
3	^{Tetra}**B3**	500	24	25	45.6	228	9.5	>99	>99	23.5	1.20
4	^{Tetra}**B2**	500	24	40	61.3	307	12.8	>99	>99	15.4	1.28
5	^{Tetra}**B2**	500	8	50	33.5	168	21.0	93	95	10.8	1.36
6	^{Tetra}**B2**	500	4	60	26.3	132	32.9	90	92	3.2	1.69
7[d]	^{Tetra}**B2**	500	24	25	41.4	207	8.6	>99	>99	19.7	1.30
8[e]	^{Tetra}**B2**	500	24	25	27.2	136	5.7	>99	>99	13.0	1.21
9	^{Tetra}**B2**	1,000	60	25	43.9	439	7.3	>99	>99	36.5	1.22
10	^{Tetra}**B2**	2,000	120	25	37.0	740	6.2	97	>99	27.3	1.26

[a]All of the polymerizations were carried out in 50 mL autoclaves under 25 bar of CO_2 unless otherwise mentioned. Abbreviations: cat., catalyst; mon., monomer; temp, temperature; conversn, conversion. [b]Calculated by ^{1}H NMR. [c]Determined by gel permeation chromatography (GPC) in THF with a polystyrene standard. [d]Polymerization was carried out under 15 bar of CO_2. [e]40 bar of CO_2 was applied.

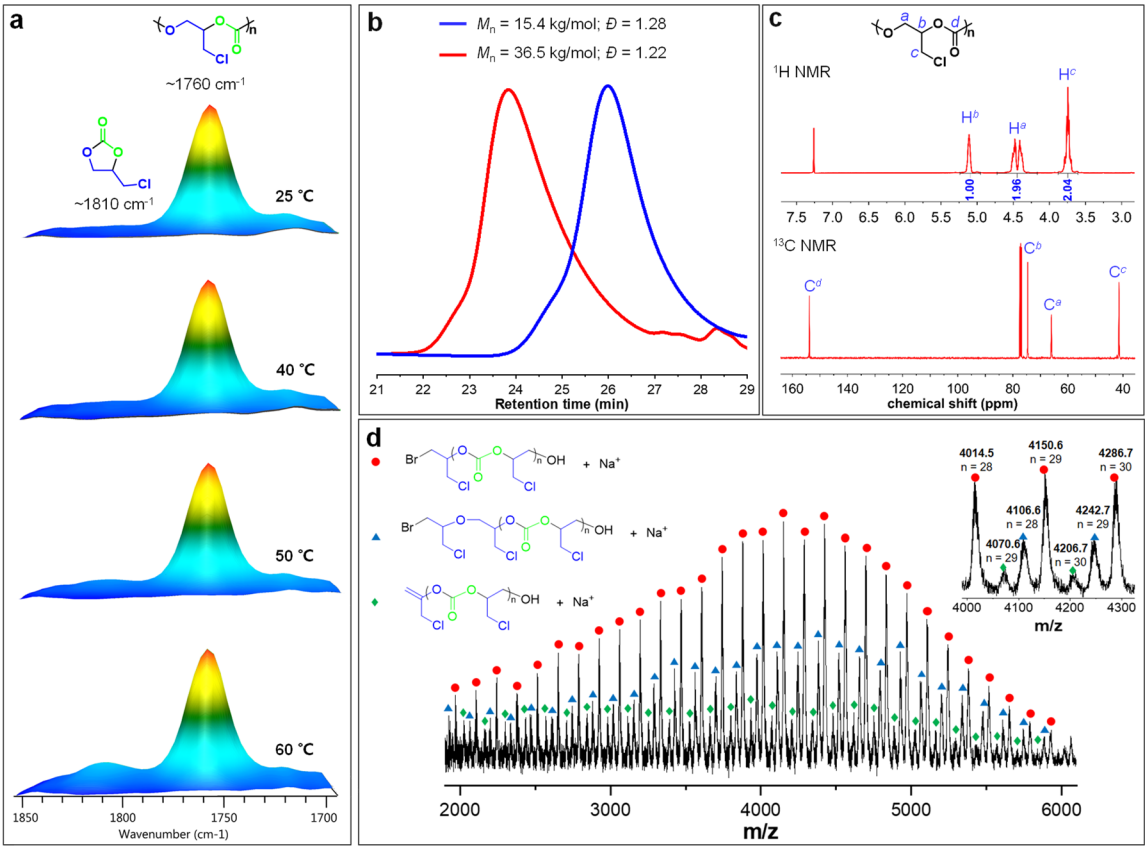

Figure 2. Characterization of ECH/CO_2 copolymerization catalyzed by ^{Tetra}**B2**. (a) *In situ* FTIR spectra monitoring the formation of polycarbonate (~1760 cm^{-1}) and cyclic carbonate (~1810 cm^{-1}) at different reaction temperatures. Reaction conditions: ECH/^{Tetra}**B2** = 500/1, solvent free, 25 bar of CO_2. (b) Representative GPC traces of PCPC samples from Table 1 (blue curve, entry 4; red curve, entry 9). (c) ^{1}H NMR (400 M, 25 °C, $CDCl_3$) and ^{13}C NMR (126 M, 25 °C, $CDCl_3$) spectra of a representative PCPC sample (entry 2, Table 1). (d) MALDI-TOF MS spectrum of the PCPC oligomer produced by ^{Tetra}**B2**.

in the product (more than 3 cycles of precipitation−dissolution; Figure 1d), and the involved harsh copolymerization conditions (0 °C) greatly limited its practical utilization.[40]

Inspired by the enzyme-mimetic multimetallic catalysis,[44−46] herein, we provide simple, practicable organoboron catalysts for the highly selective copolymerization of ECH and CO_2 under mild conditions. The organoboron catalysts composed of four Lewis acidic 9-borabicyclo[3.3.1]nonane (9-BBN) centers and a central quaternary ammonium halide (Figure 1e) can be facilely synthesized using low-cost and commercially available chemicals in nearly quantitative yield via a two-step procedure. The catalysts show >99% polymer selectivity and >99% carbonate linkages in ECH/CO_2 copolymerization under mild conditions (25−40 °C, 25 bar of CO_2), affording PCPCs with the highest molecular weight of 36.5 kg/mol and glass transition temperature of 45.4 °C reported so far. A thermodynamic study indicated that the difference in the energy of activation for cPC vs PCPC is 60.7 kJ/mol (ΔE_a) for our metal-free catalyst, 15.3 kJ/mol higher than the value obtained using the salen-Co(III) complex (ΔE_a = 45.4 kJ/

https://dx.doi.org/10.1021/jacs.0c12425
J. Am. Chem. Soc. 2021, 143, 3455−3465

mol).[40] A cyclically sequential copolymerization mechanism was rationally proposed and verified by multiple experimental methods as well as density functional theory (DFT) calculations. The metal-free feature, outstanding catalytic performance under mild conditions, and no trouble with chromaticity for the produced polymers imply that the catalysts are practical candidates to advance the challenging ECH/CO_2 copolymerization.

RESULTS AND DISCUSSION

Catalyst Synthesis and Characterization. The chemical structures of our catalysts ^{Tetra}**B1**, ^{Tetra}**B2**, and ^{Tetra}**B3** featuring four Lewis acidic BBN centers and a central quaternary ammonium halide (Cl^-, Br^-, and I^-, respectively) are provided in Figure 1e. The synthetic methodology is simple and efficient with nearly quantitative yields in two steps (Figure S1).[47] The first step is the synthesis of tetraallylammonium halides via quaternization of triallylamine with allyl halides (or treatment by ion-exchange resin). Next, hydroboration of the tetraallylammonium halides with 4.2 equiv of 9-BBN afforded the targeted metal-free catalysts as white solid powders. Given the extreme simplicity of the methodology and ease of handing, all of the catalysts could be prepared readily on a 100 g scale from commercially available, inexpensive starting materials. All of these catalysts were well-characterized by high-resolution mass spectra and NMR spectra (see the Supporting Information). In the presence of *N*,*N*-dimethylformamide (DMF), single crystals of suitable quality could be obtained for single-crystal X-ray diffraction tests. The crystal structure of ^{Tetra}**B2** is shown in Figure 1f, wherein the molecule of ^{Tetra}**B2**·4DMF adopts a pinwheel-shaped geometry, and each boron center is strongly coordinated by a DMF molecule. The four boron centers are linked to the central N^+ by the soft trimethylene arms with B···N^+ distances and B−N^+−B angles in the ranges of 5.047−5.282 Å and 85.2−99.4°, respectively. Given that each boron center is occupied by a DMF molecule, the nucleophilic Br^- hangs adjacent to the central N^+ via a Coulombic interaction with a Br^-···N^+ distance of 4.557 Å (for detailed information, see Table S1).

ECH/CO_2 Copolymerization Studies. We began our investigation with an evaluation of the influence of the initiator anions Cl^-, Br^-, and I^- on the catalytic performance for ECH/CO_2 copolymerization, and the results are collected in Table 1. As is shown, the utilization of ^{Tetra}**B1** featuring the Cl^- gave a 36.1% conversion (turnover frequency, TOF = 7.5 h^{-1}) in 24 h at 25 °C and 25 bar of CO_2 pressure (ECH/^{Tetra}**B1** = 500/1 mole ratio), affording PCPC with a M_n value of 16.3 kg/mol and a narrow polydispersity ($Đ$ = 1.19) (Table 1, entry 1). In lieu of ^{Tetra}**B1** with Cl^-, catalysts ^{Tetra}**B2** with Br^- and ^{Tetra}**B3** with I^- resulted in gradually increased reaction rates, and conversions of 39.6% (TOF = 8.3 h^{-1}, Table 1, entry 2) and 45.6% (TOF = 9.5 h^{-1}, Table 1, entry 3) were achieved, respectively. It should be noted that, under these conditions, >99% polymer selectivity and >99% carbonate linkages were achieved (Figures S2−S4). Moreover, the uncolored PCPC sample could be easily obtained by only one precipitation in methanol (Figure 1g), and the efficient removal of the catalyst residue was manifested by elemental analysis (see the Supporting Information), which is in marked contrast to the chromatic sample catalyzed by **Salen-Co** even after three cycles of dissolution−precipitation (Figure 1d).[40]

A representative *in situ* fourier transform infrared spectroscopy (FTIR) three-dimensional stack plot of ^{Tetra}**B2**-mediated ECH/CO_2 copolymerization at 25 °C is provided in Figure 2a, which clearly confirms the exclusive polymer selectivity during the coupling reaction, wherein the characteristic absorption peak (C═O stretching vibration) of the polymer carbonate linkage at ∼1760 cm^{-1} was gradually intensified without the observation of an absorption at ∼1810 cm^{-1} assigned to cyclic carbonate. We then used ^{Tetra}**B2** as a model catalyst to investigate the effect of reaction temperature on the catalytic performance, and a trend for increasing reactivity with an increase of temperature was clearly observed. It was gratifying to find that, even when the copolymerization was performed at 40 °C, there was no evidence of cPC formation and a quantitative carbon dioxide uptake (>99% carbonate linkages) was retained for the resultant PCPC (entry 4 in Table 1, Figure 2a, and Figure S5). Notably, a GPC trace of the resultant PCPC exhibits a narrow and monomodal distribution of molar masses, as shown in Figure 2b. When the reactions were performed at 50 and 60 °C, the formation of cyclic carbonate became thermodynamically unavoidable. Nonetheless, >90% polymer selectivity and >90% carbonate linkages could still be maintained (entries 5 and 6 in Table 1, Figure 2a, and Figure S6).

The perfect alternating structure of the polymer was substantiated by the ^{1}H and ^{13}C NMR and matrix-assisted laser desorption/ionization time-of-flight mass (MALDI-TOF MS) spectra (Figure 2c,d). Figure 2c presents the ^{1}H and ^{13}C NMR spectra of the resultant polymer, wherein the integrals of H^a (CH_2), H^b (CH), and H^c (CH_2Cl) at 4.5, 5.1, and 3.7 ppm, respectively, were conformed well to 2/1/2. In the corresponding ^{13}C NMR spectrum, the peaks at 152, 76, 65, and 42 ppm could be clearly assigned to C^d (C═O), C^b (CH), C^a (CH_2), and C^c (CH_2Cl) of the alternating PCPC. The full carbonate content of PCPC in the MALDI-TOF MS in Figure 2d exhibited three series of mass populations individually separated by 136 mass units (the molar masses of the repeating unit of ECH/CO_2). The primary population (red circles) is assigned to the molecular ions with mass corresponding to the sodium adduct of the alternating copolymer with α-bromide/ω-proton end groups. The secondary population (blue triangles) reveals the occurrence of the substitution of the bromide group on the chain end by an active alkoxy anion during the polymerization process. The third population (green diamonds) is 80 mass units less than the primary population, which corresponds to the elimination of a HBr molecule that may occur during the MALDI-TOF MS analysis. Notably, the cyclization side reaction that has led to the formation of a cyclic carbonate chain end in the salen-Co(III)-mediated CO_2/ECH copolymerization was not observed in our system,[40] which confirms the efficient suppression of the occurrence of a cyclization reaction using our metal-free catalyst. All three populations validated the alternating nature of the resultant PCPC (>99% carbon dioxide uptake) and further manifested that the tetranuclear catalyst ^{Tetra}**B2** is solely selective (>99%) for alternating enchainment over ether linkage formation and cyclization.

A variation in CO_2 pressure had no influence on the polymer selectivity and alternating enchainment, and >99% polymer selectivity and quantitative carbon dioxide uptake were observed over the pressure range of 15−40 bar at room temperature. Decreasing the CO_2 pressure from 25 to 15 bar made a tiny change in activity (turnover number, TON of 198 vs 207, Table 1, entries 2 and 7), while increasing the CO_2 pressure to 40 bar resulted in a reduced activity with a TON

https://dx.doi.org/10.1021/jacs.0c12425
J. Am. Chem. Soc. 2021, 143, 3455−3465

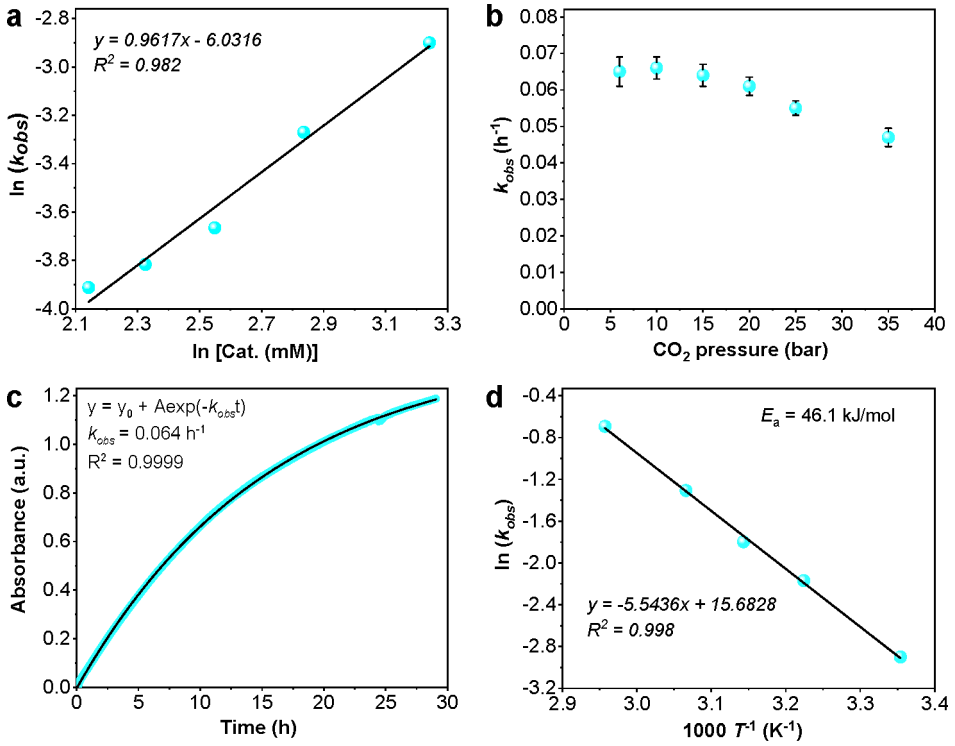

Figure 3. Kinetic measurements: (a) first order in concentration of catalyst ***Tetra*B2**; (b) zero order in CO_2 pressure; (c) first order in ECH; (d) experimental activation energy (E_a) for the formation of PCPC.

value of 136 (Table 1, entry 8), probably arising from a reduced solubility of the reagents in a supersaturated CO_2 solution, a common experimental phenomenon in the coupling reaction of epoxides/CO_2.[48,49]

The catalytic performance of ^{Tetra}**B2** under dilution conditions was also conducted. It was found that, at a low catalyst loading of 0.1 mol % (Table 1, entry 9), the catalytic activity (TOF = 7.3 h^{-1}) of ^{Tetra}**B2** was observed without any loss in polymer selectivity and carbonate content, and the afforded PCPC gave a relatively high M_n value of 36.5 kg/mol with a unimodal distribution as shown by the GPC curve (Figure 2b, red curve; for other GPC traces of PCPCs in Table 1, see Figure S7). To the best of our knowledge, this is the highest molecular weight obtained so far. The basic thermal performance of the produced PCPC examined by differential scanning calorimetry (DSC) also substantiated its status, in which a glass transition temperature value (T_g) of 45.4 °C (Figure S8), the highest value achieved to date, was observed for the copolymer of ECH and CO_2. However, no melt endothermic peak at ∼108 °C on the DSC curve was detected, indicating the atactic property of the produced PCPC.[50] Furthermore, the amorphous nature of PCPC was also demonstrated by using wide-angle X-ray diffraction, where no diffraction was observed (Figure S9). When the catalyst loading was further reduced to 0.05 mol %, the copolymerization could also proceed with a moderate rate (TOF = 6.2 h^{-1}) and >97% polymer selectivity (Table 1, entry 10).

Reaction Kinetics Study. To obtain a mechanistic insight into the copolymerization process catalyzed by our tetranuclear catalysts, we next turned our attention to the reaction kinetics (Figure 3). The *in situ* FT-IR technique was performed to explore the individual influences of ^{Tetra}**B2** loading, CO_2 pressure, and ECH concentration. For the sake of accuracy, all of the kinetic experiments were conducted with <5% ECH conversions, and the C═O stretching vibration at ∼1760 cm^{-1} of the carbonate group was monitored to calculate the initial rate coefficient, k_{obs}. The copolymerization is first order with respect to the concentration of ^{Tetra}**B2**, as was ascertained by the linear fit of ln k_{obs} to ln [^{Tetra}**B2**] from five concentrations of ^{Tetra}**B2** (8.52, 10.23, 12.80, 17.05, and 25.57 mM; Figure 3a). A zero-order dependence on CO_2 pressure was confirmed by varying the initial CO_2 pressure from 5 to 35 bar without varying other reaction conditions (ECH/^{Tetra}**B2** = 500/1, 25 °C; Figure 3b), which reveals that CO_2 incorporation is not the rate-determining step during the copolymerization process. The order in ECH concentration was determined by conducting a copolymerization with an ECH/^{Tetra}**B2** ratio of 500/1 at 25 °C and 25 bar of CO_2 pressure. The absorbance vs time data were well fitted by an exponential fit with a coefficient of determination of 0.9999, demonstrating that the copolymerization is first order with respect to ECH monomer (Figure 3c).[51] On the basis of the reaction kinetics studies, the overall rate law dependent upon all reagents can be determined as reaction rate = $k_p[^{Tetra}\mathbf{B2}]^1[\mathrm{ECH}]^1p(\mathrm{CO_2})^0$, where k_p is the propagation rate constant. The equation clearly manifests that the ring opening of ECH is the rate-determining step during the copolymerization, while highlighting that only one ^{Tetra}**B2** molecule (*i.e.*, an intramolecular synergistic catalysis) dominated the copolymerization process. Finally, by implementation of five experiments at different reaction temperatures (25, 37, 45, 53, and 65 °C), an apparent activation energy of 46.1 kJ/mol for PCPC formation was calculated from an Arrhenius plot (Figure 3d), which is 7.0 kJ/mol lower than that of the salen-Co(III)-mediated copolymerization (53.1 kJ/mol).[40] It is important to find that the difference in the energies of activation for cPC vs PCPC was determined as ΔE_a = 60.7 kJ/mol under ^{Tetra}**B2** (Figure S10), which is 15.3 kJ/mol higher than the value obtained by Lu and Darensbourg using the

https://dx.doi.org/10.1021/jacs.0c12425
J. Am. Chem. Soc. 2021, 143, 3455−3465

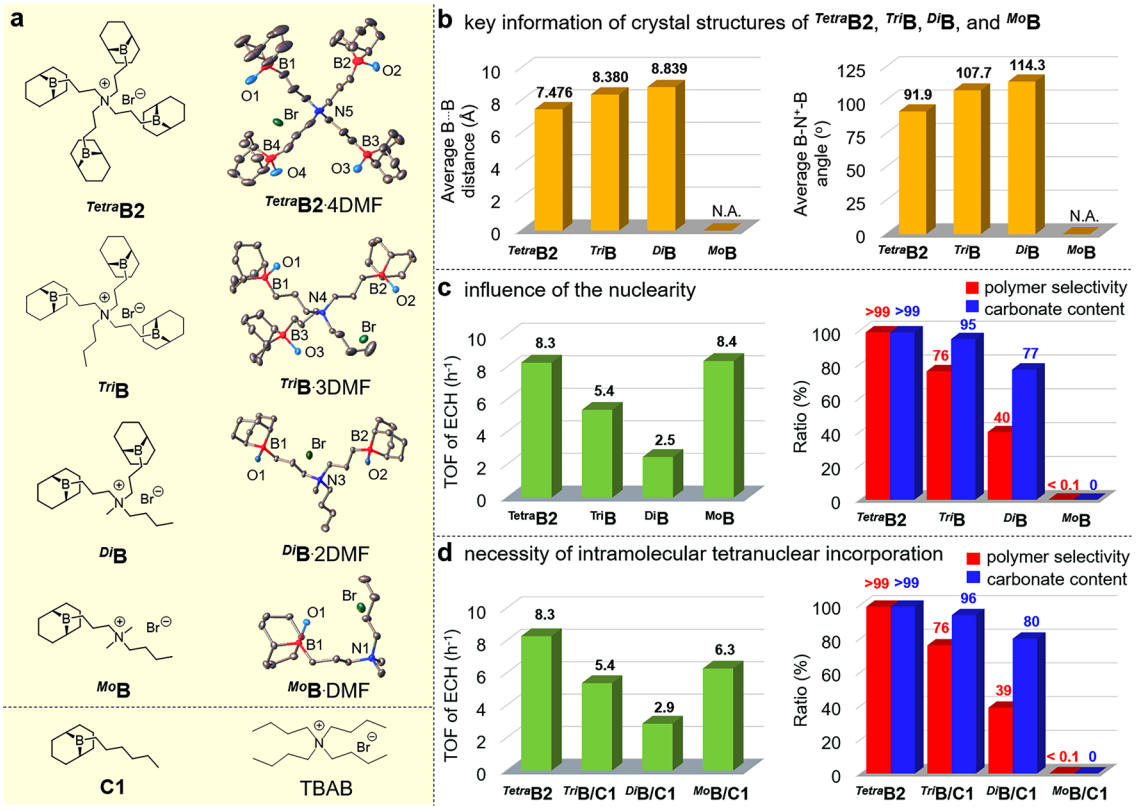

Figure 4. Control catalyst systems, crystal structures, and catalytic performances. (a) Chemical and crystal structures of control catalysts ^{Tri}**B**, ^{Di}**B**, and ^{Mo}**B** in comparison with ^{Tetra}**B2** for ECH/CO_2 copolymerization. The crystal structures of ^{Di}**B** and ^{Mo}**B** were taken from our previous studies.[52,53] All of the H atoms and solvent molecules are omitted, and the coordinated DMF are truncated for clarity. (b) Average B···B distances and B−N^+−B angles of catalysts ^{Tetra}**B2**, ^{Tri}**B**, ^{Di}**B**, and ^{Mo}**B**. N.A. denotes not applied. (c) Influence of nuclearity on catalytic activity, polymer selectivity, and carbonate content of the copolymer of ECH/CO_2. (d) Catalytic performances of the experiments using four kinds of binary control catalyst systems (^{Tri}**B**/**C1**, ^{Di}**B**/**C1**, ^{Mo}**B**/**C1**, and **C1**/TBAB), where each binary system has an intermolecular B/N^+ ratio of 4 to verify the necessity of intramolecular tetranuclear incorporation for ^{Tetra}**B2**. All control experiments were conducted in neat ECH with a catalyst loading of 0.2 mol % at 25 °C and 25 bar of CO_2 for 24 h.

salen-Co(III) complex (ΔE_a = 45.4 kJ/mol).[40] This comparative results shed light on the high polymer selectivity at enhanced temperature using our organoboron catalysts, and the rare tolerance of temperature encouraged us to probe the structure−property relationships of our catalysts, as detailed in the next section.

Control Catalyst Systems and Polymerizations. With an aim to clarifying the structure−performance relationships of our intramolecular tetranuclear catalyst (taking ^{Tetra}**B2** as a model), we synthesized a series of control catalysts that have the same boron centers, trimethylene arms between B and N^+, and initiator Br^- to ^{Tetra}**B2**. The chemical structures of these control catalysts, including the intramolecular trinuclear catalyst ^{Tri}**B**, dinuclear catalyst ^{Di}**B**, and mononuclear catalyst ^{Mo}**B**, are shown in Figure 4a. For unambiguous comparison, the crystal structures of these catalysts were also measured and are provided in Figure 4a (the crystal structures of ^{Di}**B** and ^{Mo}**B** were taken from our previous studies;[52,53] for detailed crystal information on ^{Tri}**B**, see Table S2). The key information on average B···B distances and B−N^+−B angles of ^{Tetra}**B2**·4DMF, ^{Tri}**B**·3DMF, ^{Di}**B**·2DMF, and ^{Mo}**B**·DMF are given in Figure 4b. It is clearly found that the average B···B distance and B−N^+−B angle increased from 7.476 Å/91.9° for ^{Tetra}**B2**·4DMF to 8.380 Å/107.7° for ^{Tri}**B**·3DMF and 8.839 Å/114.3° for ^{Di}**B**·2DMF with a decrease in boron centers.

With the aim of demonstrating the validity of the ^{Tetra}**B2** design that incorporates four boron centers in the molecule, we carried out a set of control experiments using tetranuclear ^{Tetra}**B2**, trinuclear catalyst ^{Tri}**B**, dinuclear catalyst ^{Di}**B**, and mononuclear catalyst ^{Mo}**B**, respectively, with a catalyst loading of 0.2 mol % at 25 °C and 25 bar of CO_2 pressure. The comparative results indicated that when the number of boron centers in the organoboron catalysts were reduced from four (^{Tetra}**B2**) to three (^{Tri}**B**), two (^{Di}**B**), and one (^{Mo}**B**), a dramatic reduction in catalytic activity, polymer selectivity, and carbonate content were observed (Figure 4c and Table S3). For example, catalyst ^{Tri}**B** with one boron center less than ^{Tetra}**B2** exhibited a much lower activity of 5.4 h^{-1}, affording PCPC with 76% polymer selectivity and 95% carbonate linkages. On a further decrease in the intramolecular boron centers to two (^{Di}**B**), the dinuclear catalyst presented an inferior activity of 2.5 h^{-1} and a poorer control of ECH/CO_2 copolymerization with only 40% polymer selectivity and 77% carbonate content. In sharp contrast, the mononuclear catalyst ^{Mo}**B** showed activity comparative to that of ^{Tetra}**B2**, but cPC was the sole product.[52] These control experiments manifest that the proximity of the boron centers could provide higher reactivity, selectivity, and carbonate content for the copolymerization, thus substantiating the necessity of our tetranuclear organoboron catalyst design. In addition, the validity of the ^{Tetra}**B2** design was also manifested by the copolymerization of

https://dx.doi.org/10.1021/jacs.0c12425
J. Am. Chem. Soc. 2021, 143, 3455−3465

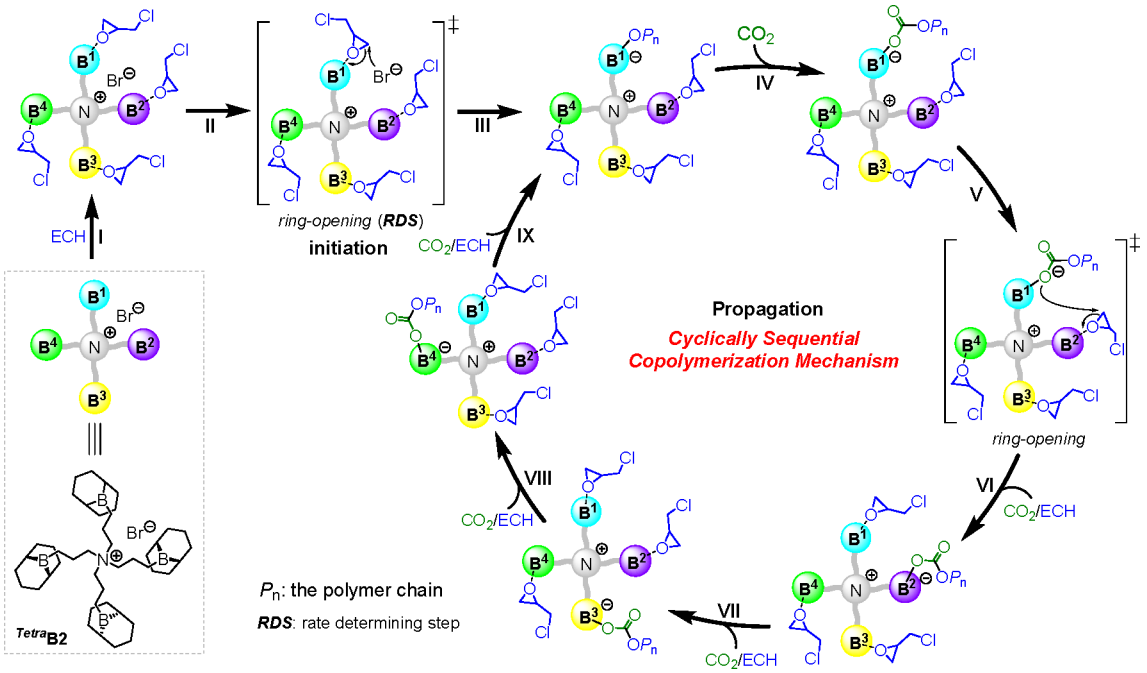

Figure 5. Proposed cyclically sequential copolymerization mechanism of ECH and CO_2 in the presence of ^{Tetra}**B2**.

CO_2 with the benchmark epoxides PO (Table S4) and CHO (Table S5), respectively. For PO, >99% polymer selectivity with an increase in the number of boron centers in the organoboron catalysts was observed, even though a small quantity of polyether content appeared. For CHO, ^{Tetra}**B2**, ^{Tri}**B**, ^{Di}**B**, and ^{Mo}**B** all exhibited >99% polymer selectivity and carbonate linkages. These comparative experiments explained the fact that the selective synthesis of copolymer of ECH/CO_2 is more challenging in comparison with the conventional copolymerization processes of PO/CO_2 and CHO/CO_2, highlighting the design of our tetranuclear organoboron catalysts.

We then probed the necessity of intramolecular cooperative effects between the four boron centers and ammonium bromide. Four kinds of binary catalyst systems with an intermolecular ratio of $B/N^+ = 4$ were used as control catalysts: that is, ^{Tri}**B**/**C1** (1/1 mole ratio), ^{Di}**B**/**C1** (1/2 mole ratio), ^{Mo}**B**/**C1** (1/3 mole ratio), and **C1**/tetrabutylammonium bromide (TBAB) (4/1 mole ratio). The catalytic performances of these binary catalysts were systematically compared with that of the intramolecular tetranuclear catalyst ^{Tetra}**B2** ($B/N^+ = 4$) that displayed high selectivity and activity for ECH/CO_2 copolymerization (Figure 4d and Table S3). The results indicated that a negligible synergistic effect occurred in the four intermolecular boron centers for these four kinds of control catalysts, as manifested by the following two experimental phenomena. First, the combination of the intermolecular components caused no promotion of the copolymerization behavior, including the TOF values, polymer selectivities, and carbonate contents. For example, the binary control catalyst ^{Tri}**B**/**C1** displayed a TOF value, polymer selectivity, and carbonate content of 5.4 h^{-1}, 76%, and 96%, respectively; this performance is no better than that of using ^{Tri}**B** without the addition of **C1** (TOF value 5.4 h^{-1}, polymer selectivity 76%, and carbonate content 95%, respectively). Similar trends were also found in the binary ^{Di}**B**/**C1**- and ^{Mo}**B**/**C1**-mediated ECH/CO_2 coupling reactions (Figure 4d and Table S3). The second fact is that the catalytic performances of these binary systems (^{Tri}**B**/**C1**, ^{Di}**B**/**C1**, ^{Mo}**B**/**C1**, and **C1**/TBAB, with an intermolecular ratio of $B/N^+ = 4$) were far inferior to that of ^{Tetra}**B2** which has an intramolecular B/N^+ ratio of 4. In comparison with ^{Tetra}**B2** (TOF = 8.3 h^{-1}, >99% polymer selectivity, and >99% carbonate content), a 35% decrease in TOF value (5.4 h^{-1}) and 23% decrease in polymer selectivity (76%) were obtained by using the ^{Tri}**B**/**C1** catalyst system, affording a PCPC with 96% carbonate content. When the binary ^{Di}**B**/**C1** catalyst system was used, the catalytic activity was reduced to 2.9 h^{-1}, only a third of that of ^{Tetra}**B2**; meanwhile, the polymer selectivity and carbonate content were sharply reduced to 39% and 80%, respectively. Notably, when the ^{Mo}**B**/**C1** and **C1**/TBAB catalyst systems were used, only the cyclic carbonate was obtained, though high TOFs of 6.3 and 12.5 h^{-1} were obtained, respectively (Figure 4d and Table S3). The above control experiments indicated that the integration of four boron centers and ammonium halide into one molecule was indispensable to suppress the backbiting side reactions and continuous insertion of ECH (polyether linkage) during the ECH/CO_2 copolymerization process.

Proposed Copolymerization Mechanism. On the basis of the aforementioned findings, we tentatively propose a cyclically sequential copolymerization mechanism based on catalyst ^{Tetra}**B2** in Figure 5. At the beginning, the nucleophilic Br^- was randomly interacted with the four Lewis acidic boron centers and the electropositive ammonium cation under the action of Coulomb forces.[53] Upon the coordination of Lewis basic ECH monomers to the Lewis acidic BBN centers (**I**), the nucleophilic attack of Br^- to the activated ECH on B^1, leading to the formation of an alkoxide-participated tetracoordinate B^1 center (chain initiation, rate-determining step; **II**–**III**). Due to the stabilization of the active alkoxy anion by a strong interaction with the boron center, the alkoxy backbiting reaction leading to the production of cPC was effectively suppressed. This proposal was demonstrated by the ring-opening experiment of ECH in the absence of CO_2, as the

https://dx.doi.org/10.1021/jacs.0c12425
J. Am. Chem. Soc. 2021, 143, 3455−3465

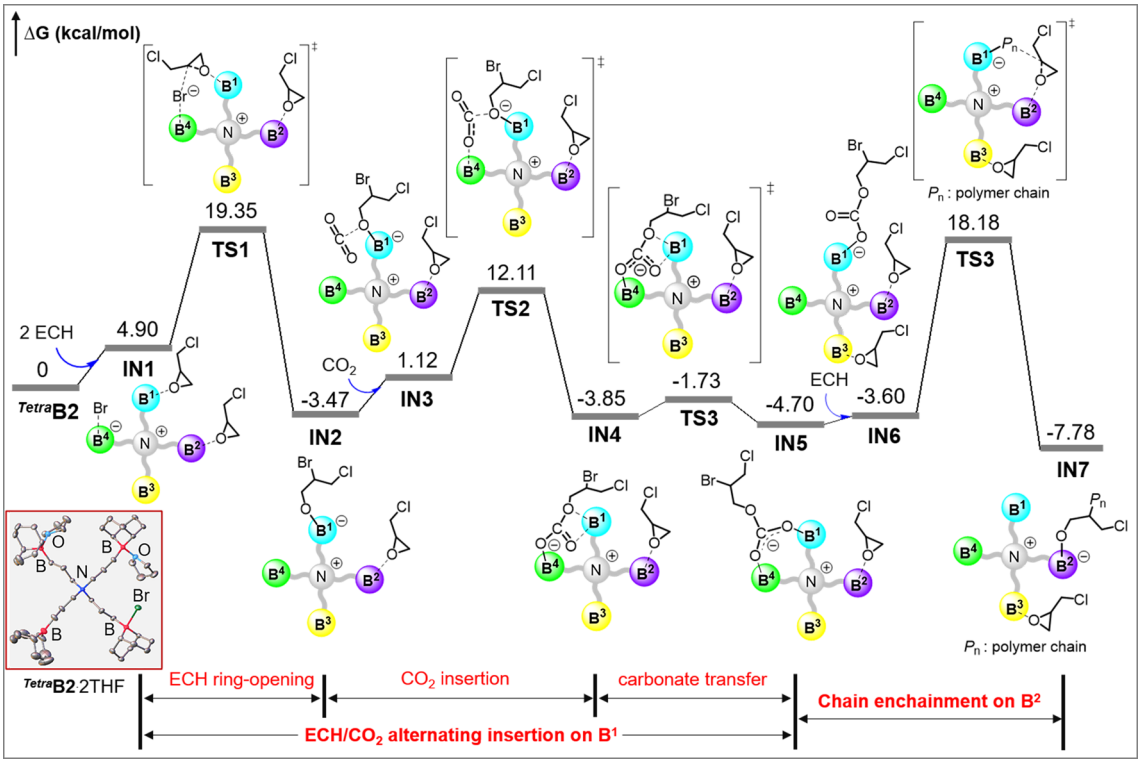

Figure 6. Gibbs free energy profile with the involved intermediates (**IN1**−**IN7**) and transition states (**TS1**−**TS3**) for ^{Tetra}**B2**-catalyzed CO_2/ECH copolymerization. The insert is the crystal structure of ^{Tetra}**B2**·2THF.

formation of an "ate" complex (a boron center was strongly coordinated with the alkoxy anion) was clearly observed by ^{1}H NMR and ^{11}B NMR spectra (Figures S11 and S12). Given that the copolymerization is zero order in CO_2 pressure, a CO_2 molecule then quickly inserts into the boron−alkoxide bond and generates the boron−carbonate bond (**IV**). The CO_2 insertion process was experimentally manifested and spectroscopically observed (Figure S13). Assisted by the Coulombic interaction with the central N^+, the weakly coordinated carbonate anion subsequently dissociates from B^1 to ring-open the already activated monomer on B^2; in the meantime, the unoccupied B^1 is coordinated by a fresh ECH molecule (**V**−**VI**). Note that the high density of intramolecular tetranuclear boron centers provides a high local concentration of Lewis acidic centers to efficiently trap the dissociated carbonate anion, thus preventing the carbonate backbiting reaction for the formation of cPC. Following this propagation manner, the repeatedly alternating insertion of ECH and CO_2 propagates from B^2 to B^3 to B^4 to B^1 in the cycle, producing the perfectly alternating ECH/CO_2 copolymer (**VII**−**IX**). It is important to note that the random chain enchainment between two proximate boron centers (e.g., from B^2 back to B^1) could be not exclusively ruled out during the copolymerization.

Computational Study. To gain a better mechanistic insight into the proposed copolymerization mechanism, computational investigations were conducted (for detailed information, see the Supporting Information), and the resultant Gibbs free energy profile with the intermediates (**IN1**−**IN7**) and transition states (**TS1**−**TS3**) involved for ^{Tetra}**B2**-catalyzed CO_2/ECH copolymerization is provided in Figure 6 (for the three-dimensional structures of **IN1**−**IN7** and **TS1**−**TS3**, see Figure S14). From the initial state to **IN1**, it was surprising to find that a favorable conformation of **IN1** only accommodates two ECH monomers on ^{Tetra}**B2**, and the coordination of the two ECH monomer to the initial state is computed to be endergonic by 4.9 kcal/mol. To demonstrate the validity of the optimized **IN1**, we cultivated the crystal of catalyst ^{Tetra}**B2** in THF solution, since THF is a non-polymerizable cyclic ether and has a coordination ability similar to that of ECH. The crystal structure of the catalyst ^{Tetra}**B2**·2THF is provided in the bottom left corner of Figure 6 (for detailed crystal data, see Table S6). As expected, the coordination of two THF molecules was clearly observed, which manifests the rationality for the optimized structure of **IN1**. Subsequent ECH ring opening by the Br^- on B^4 proceeds with an activation free energy of 19.35 kcal/mol (**TS1**). Then the alkoxy anion on B^1 of **IN2** activates a CO_2 molecule with a 4.59 kcal/mol increase in energy (**IN3**), followed by the quick insertion of the activated CO_2 into the B^1−alkoxy bond under the synergistic effect of B^1 and B^4 to afford **IN4** by overcoming an energy barrier of 10.99 kcal/mol (**TS2** to **IN4**). The following chain propagation involves a repositioning of the carbonate anion, leading to the formation of **IN5**, where the carbonate-bridged B^1 and B^4 could cooperatively stabilize the active carbonate chain end (Figure S14). These two steps are calculated to be exergonic by 0.85 kcal/mol, implying that the joint stabilization of the carbonate anion by B^4 and B^1 is more favored. After the coordination of an additional ECH monomer on B^3 (**IN5** to **IN6**), the ring opening of the activated ECH monomer on B^2 by the carbonated anion (which has a weak electrostatic interaction with B^1) leads to the formation of intermediate **IN7** with alkoxy-bonded B^2, releasing 7.78 kcal/mol free energy in comparison with the initial state. The aforementioned alternating enchainment ECH/CO_2 takes place cyclically to give the final PCPC product.

https://dx.doi.org/10.1021/jacs.0c12425
J. Am. Chem. Soc. 2021, 143, 3455−3465

CONCLUSIONS

In summary, kinds of bifunctional tetranuclear catalysts composed of four intramolecular Lewis acid centers and one ammonium salt for the highly selective copolymerization of ECH and CO_2 were synthesized in ~100% yields by employing a simple two-step synthetic procedure. The well-defined tetranuclear compounds achieve >99% polymer selectivity in ECH/CO_2 copolymerization within a broad temperature window of 25−40 °C, affording a perfectly alternating polycarbonate (>99%) with the highest molecular weight of 36.5 kg/mol and glass transition temperature of 45.4 °C reported to date. A combination of multiple experimental methods and density functional theory calculations provided mechanistic insights into the copolymerization, wherein the synergy among the intramolecular four boron centers plays a crucial role in suppressing the formation of a cyclic carbonate byproduct and ether linkage. The cyclically sequential polymerization manner along with a detailed understanding of the synergistic effect among the multinuclear borane centers should be beneficial for the design of novel multicentric catalyst systems.

ASSOCIATED CONTENT

Supporting Information

The Supporting Information is available free of charge at https://pubs.acs.org/doi/10.1021/jacs.0c12425.

Experimental procedures, characterization of all compounds, control polymerizations, DFT computational data, and crystallographic data for ^{Tetra}**B2**·4DMF (CCDC 1974842), ^{Tri}**B**·3DMF (CCDC 1974839), and ^{Tetra}**B2**·2THF (CCDC 2041735) (PDF)

Accession Codes

CCDC 1974839, 1974842, and 2041735 contain the supplementary crystallographic data for this paper. These data can be obtained free of charge via www.ccdc.cam.ac.uk/data_request/cif, or by emailing data_request@ccdc.cam.ac.uk, or by contacting The Cambridge Crystallographic Data Centre, 12 Union Road, Cambridge CB2 1EZ, UK; fax: +44 1223 336033.

AUTHOR INFORMATION

Corresponding Author

Guang-Peng Wu − *MOE Laboratory of Macromolecular Synthesis and Functionalization, Key Laboratory of Adsorption and Separation Materials & Technologies of Zhejiang Province, Department of Polymer Science and Engineering, Zhejiang University, Hangzhou 310027, People's Republic of China;* orcid.org/0000-0001-8935-964X; Email: gpwu@zju.edu.cn

Authors

Guan-Wen Yang − *MOE Laboratory of Macromolecular Synthesis and Functionalization, Key Laboratory of Adsorption and Separation Materials & Technologies of Zhejiang Province, Department of Polymer Science and Engineering, Zhejiang University, Hangzhou 310027, People's Republic of China;* orcid.org/0000-0003-2471-2953

Cheng-Kai Xu − *MOE Laboratory of Macromolecular Synthesis and Functionalization, Key Laboratory of Adsorption and Separation Materials & Technologies of Zhejiang Province, Department of Polymer Science and Engineering, Zhejiang University, Hangzhou 310027, People's Republic of China*

Rui Xie − *MOE Laboratory of Macromolecular Synthesis and Functionalization, Key Laboratory of Adsorption and Separation Materials & Technologies of Zhejiang Province, Department of Polymer Science and Engineering, Zhejiang University, Hangzhou 310027, People's Republic of China*

Yao-Yao Zhang − *MOE Laboratory of Macromolecular Synthesis and Functionalization, Key Laboratory of Adsorption and Separation Materials & Technologies of Zhejiang Province, Department of Polymer Science and Engineering, Zhejiang University, Hangzhou 310027, People's Republic of China;* orcid.org/0000-0002-8031-9139

Xiao-Feng Zhu − *MOE Laboratory of Macromolecular Synthesis and Functionalization, Key Laboratory of Adsorption and Separation Materials & Technologies of Zhejiang Province, Department of Polymer Science and Engineering, Zhejiang University, Hangzhou 310027, People's Republic of China*

Complete contact information is available at: https://pubs.acs.org/10.1021/jacs.0c12425

Notes

The authors declare no competing financial interest.

ACKNOWLEDGMENTS

This work was supported by the Zhejiang Provincial Natural Science Foundation of China (R21B040004) and the National Natural Science Foundation of China (Grants 91956123 and 51973186). The authors thank Prof. Xiaochao Shi from Shanghai University for helpful assistance in NMR measurements.

REFERENCES

(1) Artz, J.; Muller, T. E.; Thenert, K.; Kleinekorte, J.; Meys, R.; Sternberg, A.; Bardow, A.; Leitner, W. Sustainable Conversion of Carbon Dioxide: An Integrated Review of Catalysis and Life Cycle Assessment. *Chem. Rev.* **2018**, *118*, 434−504.

(2) Zhu, Y.; Romain, C.; Williams, C. K. Sustainable polymers from renewable resources. *Nature* **2016**, *540*, 354−362.

(3) Liu, Q.; Wu, L.; Jackstell, R.; Beller, M. Using carbon dioxide as a building block in organic synthesis. *Nat. Commun.* **2015**, *6*, 5933.

(4) Aresta, M.; Dibenedetto, A.; Angelini, A. Catalysis for the valorization of exhaust carbon: from CO_2 to chemicals, materials, and fuels. technological use of CO_2. *Chem. Rev.* **2014**, *114*, 1709−1742.

(5) Nakano, R.; Ito, S.; Nozaki, K. Copolymerization of carbon dioxide and butadiene via a lactone intermediate. *Nat. Chem.* **2014**, *6*, 325−331.

(6) Appel, A. M.; Bercaw, J. E.; Bocarsly, A. B.; Dobbek, H.; DuBois, D. L.; Dupuis, M.; Ferry, J. G.; Fujita, E.; Hille, R.; Kenis, P. J.; Kerfeld, C. A.; Morris, R. H.; Peden, C. H.; Portis, A. R.; Ragsdale, S. W.; Rauchfuss, T. B.; Reek, J. N.; Seefeldt, L. C.; Thauer, R. K.; Waldrop, G. L. Frontiers, opportunities, and challenges in biochemical and chemical catalysis of CO_2 fixation. *Chem. Rev.* **2013**, *113*, 6621−6658.

(7) Grignard, B.; Gennen, S.; Jerome, C.; Kleij, A. W.; Detrembleur, C. Advances in the use of CO_2 as a renewable feedstock for the synthesis of polymers. *Chem. Soc. Rev.* **2019**, *48*, 4466−4514.

(8) Zhang, X.; Fevre, M.; Jones, G. O.; Waymouth, R. M. Catalysis as an Enabling Science for Sustainable Polymers. *Chem. Rev.* **2018**, *118*, 839−885.

(9) Hu, S.; Zhao, J.; Zhang, G.; Schlaad, H. Macromolecular Architectures through Organocatalysis. *Prog. Polym. Sci.* **2017**, *74*, 34−77.

(10) Inoue, S.; Koinuma, H.; Tsuruta, T. Copolymerization of carbon dioxide and epoxide. *J. Polym. Sci., Part B: Polym. Lett.* **1969**, *7*, 287−292.
(11) Inoue, S.; Koinuma, H.; Tsuruta, T. Copolymerization of carbon dioxide and epoxide with organometallic compounds. *Makromol. Chem.* **1969**, *130*, 210−220.
(12) Huang, J.; Worch, J. C.; Dove, A. P.; Coulembier, O. Update and Challenges in Carbon Dioxide-Based Polycarbonate Synthesis. *ChemSusChem* **2020**, *13*, 469−487.
(13) Lu, X.-B.; Darensbourg, D. J. Cobalt catalysts for the coupling of CO_2 and epoxides to provide polycarbonates and cyclic carbonates. *Chem. Soc. Rev.* **2012**, *41*, 1462−1484.
(14) Kember, M. R.; Buchard, A.; Williams, C. K. Catalysts for CO_2/epoxide copolymerisation. *Chem. Commun.* **2011**, *47*, 141−163.
(15) Klaus, S.; Lehenmeier, M. W.; Anderson, C. E.; Rieger, B. Recent advances in CO_2/epoxide copolymerization-New strategies and cooperative mechanisms. *Coord. Chem. Rev.* **2011**, *255*, 1460−1479.
(16) Darensbourg, D. J. Making plastics from carbon dioxide: Salen metal complexes as catalysts for the production of polycarbonates from epoxides and CO_2. *Chem. Rev.* **2007**, *107*, 2388−2410.
(17) Coates, G. W.; Moore, D. R. Discrete metal-based catalysts for the copolymerization CO_2 and epoxides: Discovery, reactivity, optimization, and mechanism. *Angew. Chem., Int. Ed.* **2004**, *43*, 6618−6639.
(18) Cheng, M.; Lobkovsky, E. B.; Coates, G. W. Catalytic Reactions Involving C1 Feedstocks: New High-Activity Zn(II)-Based Catalysts for the Alternating Copolymerization of Carbon Dioxide and Epoxides. *J. Am. Chem. Soc.* **1998**, *120*, 11018−11019.
(19) Cohen, C. T.; Chu, T.; Coates, G. W. Cobalt catalysts for the alternating copolymerization of propylene oxide and carbon dioxide: Combining high activity and selectivity. *J. Am. Chem. Soc.* **2005**, *127*, 10869−10878.
(20) Lu, X.-B.; Shi, L.; Wang, Y.-M.; Zhang, R.; Zhang, Y. J.; Peng, X. J.; Zhang, Z. C.; Li, B. Design of highly active binary catalyst systems for CO_2/epoxide copolymerization: Polymer selectivity, enantioselectivity, and stereochemistry control. *J. Am. Chem. Soc.* **2006**, *128*, 1664−1674.
(21) Ren, W.-M.; Liu, Z.-W.; Wen, Y.-Q.; Zhang, R.; Lu, X.-B. Mechanistic Aspects of the Copolymerization of CO_2 with Epoxides Using a Thermally Stable Single-Site Cobalt(III) Catalyst. *J. Am. Chem. Soc.* **2009**, *131*, 11509−11518.
(22) Jutz, F.; Buchard, A.; Kember, M. R.; Fredriksen, S. B.; Williams, C. K. Mechanistic Investigation and Reaction Kinetics of the Low-Pressure Copolymerization of Cyclohexene Oxide and Carbon Dioxide Catalyzed by a Dizinc Complex. *J. Am. Chem. Soc.* **2011**, *133*, 17395−17405.
(23) Kember, M. R.; Williams, C. K. Efficient magnesium catalysts for the copolymerization of epoxides and CO_2; using water to synthesize polycarbonate polyols. *J. Am. Chem. Soc.* **2012**, *134*, 15676−15679.
(24) Deacy, A. C.; Moreby, E.; Phanopoulos, A.; Williams, C. K. Co(III)/Alkali-Metal(I) Heterodinuclear Catalysts for the Ring-Opening Copolymerization of CO_2 and Propylene Oxide. *J. Am. Chem. Soc.* **2020**, *142*, 19150−19160.
(25) Nakano, K.; Kobayashi, K.; Nozaki, K. Tetravalent Metal Complexes as a New Family of Catalysts for Copolymerization of Epoxides with Carbon Dioxide. *J. Am. Chem. Soc.* **2011**, *133*, 10720−10723.
(26) Wang, Y.; Qin, Y.; Wang, X.; Wang, F. Trivalent Titanium Salen Complex: Thermally Robust and Highly Active Catalyst for Copolymerization of CO_2 and Cyclohexene Oxide. *ACS Catal.* **2015**, *5*, 393−396.
(27) Cao, H.; Qin, Y.; Zhuo, C.; Wang, X.; Wang, F. Homogeneous Metallic Oligomer Catalyst with Multisite Intramolecular Cooperativity for the Synthesis of CO_2-Based Polymers. *ACS Catal.* **2019**, *9*, 8669−8676.
(28) Wang, Y.; Darensbourg, D. J. Carbon dioxide-based functional polycarbonates: Metal catalyzed copolymerization of CO_2 and epoxides. *Coord. Chem. Rev.* **2018**, *372*, 85−100.
(29) Muthuraj, R.; Mekonnen, T. Recent progress in carbon dioxide (CO_2) as feedstock for sustainable materials development: Co-polymers and polymer blends. *Polymer* **2018**, *145*, 348−373.
(30) Deacy, A. C.; Kilpatrick, A. F. R.; Regoutz, A.; Williams, C. K. Understanding metal synergy in heterodinuclear catalysts for the copolymerization of CO_2 and epoxides. *Nat. Chem.* **2020**, *12*, 372−380.
(31) von der Assen, N.; Bardow, A. Life cycle assessment of polyols for polyurethane production using CO_2 as feedstock: insights from an industrial case study. *Green Chem.* **2014**, *16*, 3272−3280.
(32) Lu, X.-B.; Ren, W.-M.; Wu, G.-P. CO_2 Copolymers from Epoxides: Catalyst Activity, Product Selectivity, and Stereochemistry Control. *Acc. Chem. Res.* **2012**, *45*, 1721−1735.
(33) Zhang, Y.-Y.; Wu, G.-P.; Darensbourg, D. J. CO_2-based block copolymers: Present and future designs. *Trends Chem.* **2020**, *2*, 750−763.
(34) Lari, G. M.; Pastore, G.; Haus, M.; Ding, Y.; Papadokonstantakis, S.; Mondelli, C.; Pérez-Ramírez, J. Environmental and economical perspectives of a glycerol biorefinery. *Energy Environ. Sci.* **2018**, *11*, 1012−1029.
(35) Morodo, R.; Gérardy, R.; Petit, G.; Monbaliu, J.-C. M. Continuous flow upgrading of glycerol toward oxiranes and active pharmaceutical ingredients thereof. *Green Chem.* **2019**, *21*, 4422−4433.
(36) Wei, R.-J.; Zhang, X.-H.; Du, B.-Y.; Fan, Z.-Q.; Qi, G.-R. Selective production of poly(carbonate−co−ether) over cyclic carbonate for epichlorohydrin and CO_2 copolymerization via heterogeneous catalysis of Zn−Co (III) double metal cyanide complex. *Polymer* **2013**, *54*, 6357−6362.
(37) Song, P.; Guo, R.; Ma, W.; Wang, L.; Ma, F.; Wang, R. Synthesis of CO_2-based polycarbonate-g-polystyrene copolymers via NMRP. *Chem. Commun.* **2020**, *56*, 9493−9496.
(38) Shen, Z. Q.; Chen, X. H.; Zhang, Y. F. New Catalytic-systems for the fixation of carbon-dioxide. 2. synthesis of high-molecular-weight epichlorohydrin carbon-dioxide copolymer with rare-earth phosphonates triisobutyl-aluminum systems. *Macromol. Chem. Phys.* **1994**, *195*, 2003−2011.
(39) Sudakar, P.; Sivanesan, D.; Yoon, S. Copolymerization of Epichlorohydrin and CO_2 Using Zinc Glutarate: An Additional Application of ZnGA in Polycarbonate Synthesis. *Macromol. Rapid Commun.* **2016**, *37*, 788−793.
(40) Wu, G.-P.; Wei, S.-H.; Ren, W.-M.; Lu, X.-B.; Xu, T.-Q.; Darensbourg, D. J. Perfectly Alternating Copolymerization of CO_2 and Epichlorohydrin Using Cobalt(III)-Based Catalyst Systems. *J. Am. Chem. Soc.* **2011**, *133*, 15191−15199.
(41) Reiter, M.; Vagin, S.; Kronast, A.; Jandl, C.; Rieger, B. A Lewis acid beta-diiminato-zinc-complex as all-rounder for co- and terpolymerisation of various epoxides with carbon dioxide. *Chem. Sci.* **2017**, *8*, 1876−1882.
(42) Darensbourg, D. J.; Fitch, S. B. An Exploration of the Coupling Reactions of Epoxides and Carbon Dioxide Catalyzed by Tetramethyltetraazaannulene Chromium(III) Derivatives: Formation of Copolymers versus Cyclic Carbonates. *Inorg. Chem.* **2008**, *47*, 11868−11878.
(43) Allen, S. D.; Byrne, C. M.; Coates, G. W.; Bozell, J.; Patel, M. In *Feedstocks for the future*; Bozell, J. J., Patel, M. K., Eds.; American Chemical Society: Washington, DC, 2006; Vol. *921*, p 123.
(44) McInnis, J. P.; Delferro, M.; Marks, T. J. Multinuclear Group 4 Catalysis: Olefin Polymerization Pathways Modified by Strong Metal-Metal Cooperative Effects. *Acc. Chem. Res.* **2014**, *47*, 2545−2557.
(45) Park, J.; Hong, S. Cooperative bimetallic catalysis in asymmetric transformations. *Chem. Soc. Rev.* **2012**, *41*, 6931−6943.
(46) Jacobsen, E. N. Asymmetric catalysis of epoxide ring opening reactions. *Acc. Chem. Res.* **2000**, *33*, 421−431.
(47) Yang, G.-W.; Zhang, Y.-Y.; Xie, R.; Wu, G.-P. Scalable Bifunctional Organoboron Catalysts for Copolymerization of CO_2

https://dx.doi.org/10.1021/jacs.0c12425
J. Am. Chem. Soc. 2021, 143, 3455−3465

and Epoxides with Unprecedented Efficiency. *J. Am. Chem. Soc.* **2020**, *142*, 12245−12255.
(48) Huang, R.; Rintjema, J.; González-Fabra, J.; Martín, E.; Escudero-Adán, E. C.; Bo, C.; Urakawa, A.; Kleij, A. W. Deciphering key intermediates in the transformation of carbon dioxide into heterocyclic products. *Nat. Catal.* **2019**, *2*, 62−70.
(49) Jutz, F.; Buchard, A.; Kember, M. R.; Fredriksen, S. B.; Williams, C. K. Mechanistic Investigation and Reaction Kinetics of the Low-Pressure Copolymerization of Cyclohexene Oxide and Carbon Dioxide Catalyzed by a Dizinc Complex. *J. Am. Chem. Soc.* **2011**, *133*, 17395−17405.
(50) Wu, G.-P.; Xu, P.-X.; Lu, X.-B.; Zu, Y.-P.; Wei, S.-H.; Ren, W.-M.; Darensbourg, D. J. Crystalline CO_2 Copolymer from Epichlorohydrin via Co(III)-Complex-Mediated Stereospecific Polymerization. *Macromolecules* **2013**, *46*, 2128−2133.
(51) Trott, G.; Garden, J. A.; Williams, C. K. Heterodinuclear zinc and magnesium catalysts for epoxide/CO_2 ring opening copolymerizations. *Chem. Sci.* **2019**, *10*, 4618−4627.
(52) Zhang, Y.-Y.; Yang, G.-W.; Xie, R.; Yang, L.; Li, B.; Wu, G.-P. Scalable, Durable, and Recyclable Metal-Free Catalysts for Highly-Efficient Conversion of CO_2 to Cyclic Carbonates. *Angew. Chem., Int. Ed.* **2020**, *59*, 23291−23298.
(53) Yang, G.-W.; Zhang, Y.-Y.; Xie, R.; Wu, G.-P. High-Activity Organocatalysts for Polyether Synthesis via Intramolecular Ammonium Cation Assisted S_N2 Ring-Opening Polymerization. *Angew. Chem., Int. Ed.* **2020**, *59*, 16910−16917.

https://dx.doi.org/10.1021/jacs.0c12425
J. Am. Chem. Soc. 2021, 143, 3455−3465